Physics – Uspekhi **56** (1) 93 – 102 (2013)

METHODOLOGICAL NOTES PACS numbers: **02.70. – c**, **05.45. – a**, **64.60. – i**

Critical phenomena far from equilibrium

E N Rumanov

DOI: 10.3367/UFNe.0183.201301f.0103

Contents

Abstract. Stationary regimes of active systems — those in which dissipation is compensated by pumping — are considered. Approaching the bifurcation point of such a regime leads to an increase in susceptibility, with soft modes making the dominant contribution. Weak noise, which is inherent to any real system, increases. Sufficiently close to bifurcation, the amplitude of random pulsations is comparable to the average value of the fluctuating quantity, as in the case of developed turbulence. The spectrum of critical pulsations is independent of the original noise. Numerical simulation of the neighborhood of a bifurcation point is considered unreliable because of the poor reproducibility of results. Due to the high susceptibility, calculation roundings result in 'chaotic' jumps of the solution in response to a smooth change in the parameters. It is therefore necessary in the simulation process to introduce a small random function of time, white noise. The solutions of the Langevin equations obtained in this way should be processed statistically. Their properties (except for the intensity of pulsations) are independent of the noise induced. Examples of the statistical description of bifurcations are given.

1. Introduction

By an active system, we mean one that, while submerged in a heat bath, is kept far from equilibrium by a certain external action (for example, an applied voltage produces a current in a conductor). In the absence of an external action, the system relaxes to equilibrium with the heat bath. The time this takes is called the relaxation time, and, importantly, the final state is independent of what the initial state was. Switching on an interaction results in the dependence on the initial conditions and on the time scale of relaxation disappearing, leading to a steady-state regime that is the same for the entire set of initial conditions. This set forms a basin of attraction in the space of states, containing an attractor to which all the trajectories of the basin converge.

For a time-independent interaction, steady states can occur among the regimes that set in. Equilibrium can be considered a limit case of a steady-state regime in which the intensity of the external influence tends to zero. One of the characteristics of equilibrium is susceptibility, which can be defined as follows [1]. Let a system be subject to a small sinusoidal perturbation. The state of the system then changes at the same frequency, and the susceptibility is the ratio of the amplitude of this change to that of the perturbation. A similar definition applies to a steady-state far-from-equilibrium regime, in which case a small sinusoidal addition to a constant perturbation should be considered.

As system and/or perturbation parameters change, the steady-state regime can lose its stability and transform into a different regime. For point-like systems, the space of states is finite dimensional, and the point corresponding to a steady state in this space is a limit one. The proximity of bifurcation often suggests a contraction, at least in one direction, of the distance of this point from the boundary of its attraction basin. If the state is somewhat away from the limit point in this direction, the 'force' that returns the system to its original regime is small. For equilibrium systems, there is a visual way to explain why this is the case. Corresponding to a stable point is a minimum of a (thermodynamic) potential, and to an unstable point, a maximum (in the given direction). Bringing the two points together decreases the potential gradient (i.e., force), and thus creates a situation close to indifferent equilibrium (for both point-like and distributed systems). Even a small change in the perturbation causes a significant deviation from the steady-state regime under critical conditions (when the system parameters are close to the bifurcation

E N Rumanov Institute of Structural Macrokinetics and Materials Science, Russian Academy of Sciences,
ul. Akad. Osipyana 8, 142432 Chernogolovka, Moscow region, Russian Federation. E-mail: ed@ism.ac.ru

Received 24 June 2011, revised 22 December 2011
Uspekhi Fizicheskikh Nauk **183** (1) 103 – 112 (2013)
DOI: 10.3367/UFNr.0183.201301f.0103
Translated by E G Strel'chenko; edited by A M Semikhatov

point), and the deviation relaxation time increases; in other words, the susceptibility increases (primarily in its low-frequency part, because at low frequencies the system has enough time to deviate considerably before the external influence changes its direction).

Critical phenomena are due to high susceptibility and, as far as equilibrium is concerned, were first studied in connection with the liquid–vapor transition. The important results obtained then were the increase in susceptibility (in this case, compressibility) and (primarily soft-mode) density fluctuations [2] (specifically, thermal fluctuations, whose variance can be found by thermodynamic calculations). Far from the equilibrium, thermal noise often occurs (random input voltage oscillations being an example). Weak noise has no noticeable effect on the behavior of the system as long as the system parameters are far from the bifurcation point, but approaching this point causes the noise to increase due to the high susceptibility. Indeed, sufficiently deep in the critical region, the random amplitude of pulsations is comparable to the average value of the fluctuating quantity, similarly to the developed turbulence case. The steady-state regime turns out to be chaotic. The pulsation spectrum is independent of the 'core' noise and is dominated by low frequencies. The closer to the bifurcation point, the higher and sharper the low-frequency peak is. Unlike flicker noise [3], this peak disappears as the parameter values move farther and farther from their critical values.

Numerical simulation of the bifurcation region is considered unreliable due to poorly reproducible results. The number of digits is always constant, and unavoidable roundings result in smooth variations of the parameters, leading to jumps in solutions at high susceptibility. The way out, as we see it, is to bring the situation closer to experiment by adding a small random function of time (white noise) to the constant source. The solutions of the Langevin equation [4] obtained in this way are also random functions and should be processed statistically. For given values of the parameters, it is possible to find the variance of the pulsations, their frequency spectra, critical exponents, n-point correlators, etc., thus obtaining a reliable description of critical phenomena. The bifurcation theory must have a bearing on statistics.

In a real system, noise is not white in general, and its statistics are typically unknown. As the bifurcation point is approached, however, the pulsation correlation time increases and definitely exceeds the noise correlation time, with the result that any noise looks like a δ-correlated (white) one. For a complex system, especially for a distributed one, the susceptibility can be difficult to calculate; sufficiently deep in the critical region, nonlinear susceptibility is important. On the other hand, these quantities should not necessarily be used. As noted above, solutions of the Langevin equations are chaotic time series similar to what is obtained in real life experiments. If the series are sufficiently long (which means a long computation time), high accuracy can be achieved in determining bifurcation statistics.

Systems with a relatively small ($n \geqslant 3$ [5]) number of dependent variables allow chaotic solutions without noise addition (dynamical chaos). But the phase trajectories corresponding to such solutions are locally smooth and should be monitored for a long time (for example, by constructing a Poincaré map [6]) in order to detect chaos. The trajectories of the Langevin equations are Brownian. In typical cases, extending the spectral density of critical pulsations to all frequencies (up to the inverse atomic collision time) would give a temperature $\sim 10^5$ K. In fact, the spectrum falls off sharply with increasing the frequency, only soft modes are excited, and the substance remains cold. On a scale that is larger than atomic (but, normally, smaller than the system size), intense mixing occurs.

In bifurcation theory (see, e.g., Refs [7, 8]), following the spirit of the geometry of smooth maps [9], much attention is given to state space singularities, in which context exotic objects such as the 'saddle–node', 'saddle–focus', and, in the case of many dimensions, even more complex objects are introduced, which, elegant as they are, are still not observable in real life. We see below that (1) in the region of criticality, the neighborhood of a limit point becomes a chaotic attractor consisting of Brownian trajectories and (2) singularities are smeared out.

There is a large amount of literature on dynamic chaos with locally smooth trajectories (see, e.g., Ref. [10] for a review). Because noise cannot be fully eliminated in reality, the question arises: are such attractors of interest for physics? Far from bifurcation, where the susceptibility is not high, the Brownian nature of trajectories is not apparent. Our objective is to draw attention to an unusual type of *critical attractor* that becomes relevant if the parameters involved are close to the bifurcation point of a steady-state regime. A critical attractor consists of Brownian trajectories. A similar remark should be made concerning Hamiltonian systems with a saddle point in the phase space. The appearance of a 'stochastic layer' next to the separatrix [11], in fact, implies that noise cannot be neglected in this situation.

The above suggests that it is in principle possible to create devices that, given a complex natural or artificial system, can warn of the nearing bifurcation of its stationary regime (i.e., a catastrophe) based on the enhancement of soft modes in the system noise spectrum. Of course, the soft mode range is specific for each system. For example, for a continuously stirred tank reactor (CSTR), frequencies smaller than the inverse mixture residence time should be considered. In designing such a device, at least a basic understanding is needed of the processes in the system the device is intended for. Macrokinetic equations, including those for mass, momentum, and energy balance, are indispensable for this purpose.

2. Critical susceptibility

We first consider the case of a point-like system, i.e.,

$$\frac{\mathrm{d}X_i}{\mathrm{d}t} = f_i(X_1, X_2, \ldots) + y_i(t)\,, \qquad i = 1, 2, \ldots, n\,. \tag{1}$$

Here, X_i are coordinates (dependent variables), t is time, the vector field f_i depends on the coordinates and the constant force applied to the system, and y_i are small time-dependent force additions. If these additions are neglected, system (1) can have constant solutions X_i^{s} satisfying the equations

$$f_i(X_1^{\mathrm{s}}, X_2^{\mathrm{s}}, \ldots) = 0\,. \tag{2}$$

Such solutions correspond to steady-state regimes of an active system specified by the field f_i. If deviations from the steady state, $x_i = X_i - X_i^{\mathrm{s}}$, are assumed to be small, we can write the linear equations

$$\frac{\mathrm{d}x_i}{\mathrm{d}t} = -\lambda_{ik}x_k + y_i\,, \tag{3}$$

where repeated indices imply summation and $-\lambda_{ik} = \partial f_i/\partial X_k$ is the Jacobi matrix calculated at the limit point $X_i = X_i^s$ of the state space.

Close to bifurcation, the limit point is approached by the boundary of its attraction basis along at least one direction. We let X denote the coordinate corresponding to this direction; the relaxation time for deviations $x = X - X^s$ is large compared to that for the other degrees of freedom, due to the small 'restoring' force for this coordinate (bifurcation variable). Deviations for the other, fast-relaxing, coordinates are averaged, and hence, relative to x, they can be considered to be equal to the steady-state values $x_i = 0$. This leaves us with only one of Eqns (3),

$$\frac{dx}{dt} = -\lambda x + y\,. \tag{4}$$

Here, the coefficient λ plays the role of a bifurcation parameter, its value at the bifuraction point being $\lambda = 0$. The susceptibility $\sigma(\omega)$ at a frequency ω is defined as the Fourier component ratio x_ω/y_ω. According to Eqn (4),

$$\mathrm{Re}\,\sigma = \frac{\lambda}{\lambda^2+\omega^2}\,, \qquad \mathrm{Im}\,\sigma = \frac{\omega}{\lambda^2+\omega^2}\,. \tag{5}$$

As $\lambda \to 0$, both the real and imaginary parts of the susceptibility increase primarily at low frequencies, $\omega < \lambda$. The closer to the bifurcation point, the higher and sharper the low-frequency peak is.

Weak noise, an inherent feature of any real influence (as exemplified by random oscillations in an input voltage), becomes higher as the susceptibility increases. For sufficiently small λ, the amplitude of random pulsations is comparable to the average value of the fluctuating quantity (i.e., X^s), as in the case of developed turbulence. To put it another way, approaching bifurcation causes the regime to change from steady state to chaotic. As is clear from the above, for an arbitrary initiating noise, the pulsations must have a low-frequency peak in their spectrum. But in contrast to the flicker noise [3], this peak disappears as the parameters are moved away from the bifurcation point.

In the mathematical theory of bifurcations (see, e.g., Refs [7, 8]), much attention is focused on rearrangements in the state space, which are treated using the geometry of smooth maps [9]. We suppose, for example, that there are two singular points, a node and a saddle, which approach one another as the parameters are varied. According to Refs [7, 8], a saddle–node pair forms at the critical values of the parameters, after which the singularity disappears. As we have seen, including noise makes saddle–node and saddle–focus pairs (and, in higher dimensions, more complex objects) unobservable. The trajectories randomly intersect one another and, because of the increased noise, cannot even approximately be considered autonomous. A further point to emphasize is that critical chaos differs from the chaotic solutions that autonomous systems with a relatively small number of equations provide in a certain parameter range [5]. In this last case, the trajectories are locally smooth, and to see the presence of chaos, it is necessary to monitor them for some finite period of time (for example, by constructing the Poincaré map [6]). The critical trajectory turns out to be Brownian and densely covers the neighborhood of the limit point. As already noted above, however, here, in contrast to the standard Brownian motion (thermal fluctuations), only soft modes are excited. The chemically interesting fact of an increased mixing intensity (critical diffusion) should also be noted [13].

If the bifurcation is such that n variables relax anomalously slowly, we can introduce a susceptibility matrix $\sigma_{ik}(\omega)$ as the resolvent of the Jacobi matrix in Eqn (3),

$$\sigma_{ik}(\omega) = (\lambda_{ik} - \mathrm{i}\omega\delta_{ik})^{-1}\,. \tag{6}$$

Here, the exponent -1 denotes the inverse matrix. In the case of equilibrium, the variance of thermal fluctuations can be calculated by thermodynamic formulas. The coefficients λ_{ik} are expressed in terms of the derivatives of the entropy S,

$$\lambda_{ik} = -\frac{1}{2}\frac{\partial^2 S}{\partial x_i\,\partial x_k}\,, \tag{7}$$

taken at the limit point, where the entropy has a maximum. The most detailed studies have been performed on equilibrium bifurcations corresponding to continuous phase transitions. In this case, the bifurcation variable is referred to as an order parameter. Near the critical liquid–vapor transition point in the pressure–temperature plane, the bifurcation curves of a spinodal decomposition converge to the phase equilibrium line (boiling curve), forming a cusp, the end of the bistable (overheating and overcooling) region. In the neighborhood of this point, the compressibility (the susceptibility with respect to the transition order parameter, the density) is large. The theory of continuous transitions and critical phenomena under equilibrium conditions has been worked out in detail (see, e.g., Ref. [12]). We do not discuss these questions here.

3. Langevin equations

Numerical simulation cannot be considered a reliable way of studying the neighborhood of bifurcations because (1) the computed results show a lack of reasonable reproducibility; and (2) a smooth change in parameter values leads not to smooth changes but to random jumps in the solution. The reason for this is obvious: as a result of high susceptibility, roundings involved in the numerical integration of finite-difference equations cause significant changes in these solutions. The way out is to bring the problem formulation closer to the experimental situation. Random pulsations in the critical region not only are observed in numerical simulations but also are seen in experiment. Along with thermal fluctuations, nonthermal noise can be a source of such pulsations, which, in equilibrium, are due to inhomogeneities, impurities, and other factors that act to 'smear out' a continuous phase transition. In active systems, an influence is inevitably accompanied by weak noise at least, necessitating that the governing equations be augmented by a controlled noise term that makes solutions more chaotic compared to what the roundings produce in an uncontrollable way. The resulting solutions — which are random functions of time — should then be subjected to statistical processing.

Equations containing a weak random source are referred to as Langevin equations [4]. In the case of Eqn (4) alone, we take the function $y(t)$ to be white noise:

$$\langle y(t)\,y(t')\rangle = \mathrm{const}\,\delta(t-t')\,. \tag{8}$$

Random pumping gives rise to random motion near the limit point. According to Eqn (4), the correlator is

$$\langle x(t_1)\,x(t_2)\rangle = \exp\left[-\lambda(t_1+t_2)\right] \times \int_{-\infty}^{t_1} \mathrm{d}t \int_{-\infty}^{t_2} \mathrm{d}t'\,\langle y(t)\,y(t')\rangle \exp\left[\lambda(t+t')\right] \tag{9}$$

or

$$\langle x(t_1)\,x(t_2)\rangle = \frac{\text{const}}{2\lambda}\exp\left(-\lambda|t_1-t_2|\right). \tag{10}$$

The constant in Eqns (8) and (10) is $(y^2)_\omega$, where the white noise Fourier component is independent of frequency. For the Fourier components of the correlator,

$$(x^2)_\omega = \int_{-\infty}^{\infty} \langle x(t)\,x(t-t')\rangle \exp(\mathrm{i}\omega t')\,\mathrm{d}t', \tag{11}$$

we have

$$(x^2)_\omega = \frac{2\lambda}{\lambda^2+\omega^2}\langle x^2\rangle = \frac{(y^2)_\omega}{\lambda^2+\omega^2}. \tag{12}$$

Formulas (9)–(12) are identical to similar expressions for equilibrium [1]. In Ref. [1], however, the variance $\langle x^2\rangle$ is a known quantity calculated from thermodynamic formulas. For example, for the temperature, $\langle \Delta T^2\rangle = k_\mathrm{B}T^2/c_V$, where k_B is the Boltzmann constant and c_V is the specific heat at constant volume. Therefore, the constant in Eqn (8) is not arbitrary and should be chosen such that equalities (10) and (12) hold at a given variance $\langle x^2\rangle$. In the case of an active system far from equilibrium, the intensity of a random source $y(t)$ should be regarded as a specified noise component of the influence. Pulsations due to this noise are usually stronger than thermal fluctuations.

Using the Langevin equations, high-susceptibility systems can be numerically simulated in a way closely corresponding to the experimental situation. The order of actions is as follows. One or more of the equations is augmented by a weak white noise term and the resulting system is then integrated numerically over a chosen time interval, which should be large compared to the time scales of the original problem (relaxation time, etc.). This procedure is repeated for different values of the bifurcation parameter in the critical region and for a number of values of the noise intensity (spectral density). The data array (or rather a set of time series) so obtained is processed statistically. In Section 4, we consider a simple example of the numerical simulation of critical phenomena.

4. Critical attractor

Viewed from the perspective of nonlinear physics, exothermic reactions are interesting because of the feedback between temperature and the reaction rate in the sense that a reaction causes heating, which in turn accelerates the reaction. A mathematical model for processes involving such reactions should include equations with exponential sources (the reaction rate is usually activation-temperature dependent). Strong nonlinearity makes the physical picture more contrasting and new effects easier to discover. An exothermal transformation in a CSTR is described by the equations [14, 15]

$$\frac{\mathrm{d}\eta}{\mathrm{d}t} = \Phi(\eta, T) - \eta\tau^{-1}, \tag{13}$$

$$\frac{\mathrm{d}T}{\mathrm{d}t} = \frac{Q}{c}\,\Phi - \alpha(T-T_\mathrm{a}) \tag{14}$$

for the reaction product concentration (transformation depth) η and temperature T. The reaction rate in the simplest case is given by

$$\Phi = (1-\eta)k\exp\left(-\frac{E}{T}\right), \tag{15}$$

where k is a constant of dimension frequency and E the activation energy expressed in the same units as temperature. Usually, $E \gg T$. Other notations are: τ is the reactor residence time of the mixture, Q is the reaction heat, c is the specific heat, $\alpha = \tau^{-1} + \tau_\mathrm{f}^{-1}$, τ_f is the reactor cooling time under no-flow conditions, i.e., for $\tau \to \infty$, and T_a is the temperature of the heat bath and the supplied mixture.

It was noted as early as Ref. [14] that system (13), (14) exhibits bistability in the sense that depending on the initial conditions, either a cold (T_a) steady-state regime or a hot ($T - T_\mathrm{a} \approx Q/c\alpha\tau$) regime is established. It is assumed that the mixing time is small compared to τ. Instead of Eqns (13) and (14), a single second-order equation can be considered. For example, expressing η in terms of T and $\mathrm{d}T/\mathrm{d}t$ using Eqn (14), we obtain [16]

$$\ddot{T} = -\frac{\mathrm{d}V}{\mathrm{d}T} - \gamma(T,\dot{T})\dot{T} \tag{16}$$

(with the dot denoting time differentiation),

$$-\frac{\mathrm{d}V}{\mathrm{d}T} = -\frac{Q}{c\tau}\,k\exp\left(-\frac{E}{T}\right) + \left[k\exp\left(-\frac{E}{T}\right) + \frac{1}{\tau}\right]\alpha(T-T_\mathrm{a}), \tag{17}$$

$$\gamma = \alpha + \frac{1}{\tau} + k\exp\left(-\frac{E}{T}\right) - \frac{E}{T^2}\left[\alpha(T-T_\mathrm{a}) + \dot{T}\right]. \tag{18}$$

Mathematically, Eqn (16) is equivalent to the equation of motion in one dimension T for a particle of unit mass subject to potential force (17) and the friction force $-\gamma\dot{T}$. If η and T are specified at the initial instant, the initial 'velocity' $\dot{T}$ is determined by Eqn (14). The 'friction coefficient' in Eqn (18), depending on the parameters, can change sign and become negative — a feature that makes Eqn (16) similar to the Van der Pol equation [17]. Whether the inequality $\gamma < 0$ holds depends on the pumping, i.e., the material flow through the reactor.

The potential $V(T)$ has one minimum outside and three extrema (two minima and one maximum in between) inside the bistability region. The extrema $T_\mathrm{d} < T_\mathrm{m} < T_\mathrm{u}$ clearly have positions coincident with the temperatures of steady-state solutions of system (13), (14). A closer look at $V(T)$ allows us to see which of the two stable states corresponds to a deeper minimum. Let the problem parameters be taken as the Damköhler and Semenov numbers,

$$D = \tau k\exp\left(-\frac{E}{T_\mathrm{c}}\right), \qquad S = D(\alpha\tau)^{-1}, \tag{19}$$

and the scale temperature T_c be the temperature at the cusp where the bistable region in the (D, S) plane terminates (and

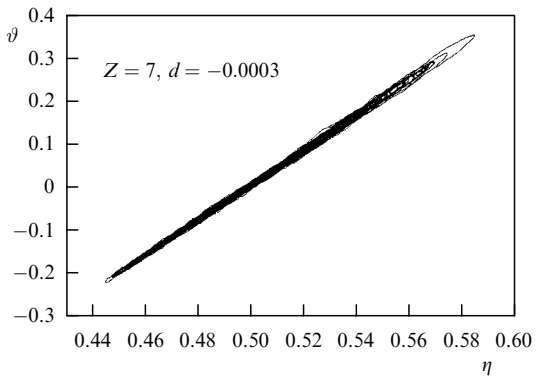

Figure 1. Overall view of the critical attractor.

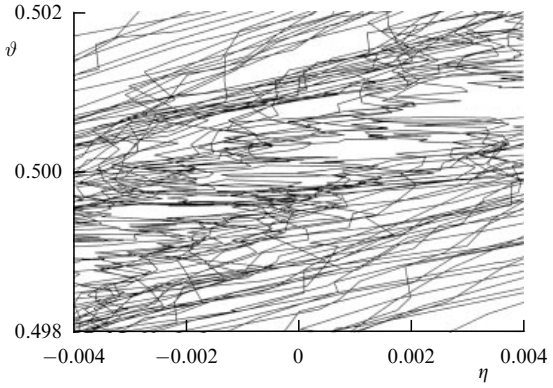

Figure 2. A magnified view (100×) of a small portion of the attractor shown in Fig. 1. The Brownian nature of the trajectory can be seen.

where all three extrema merge). It is readily seen [18] that the cusp is similar to a critical point in the pressure–temperature plane for the liquid–vapor system. The curve $V_d = V_u$ is similar to the boiling curve (phase equilibrium), and the boundaries of the bistable region are similar to spinodals. For the purposes of numerical simulation, it is useful to introduce the dimensionless temperature

$$\vartheta = \frac{E}{T_c^2}(T - T_c)\,, \qquad \exp\left(-\frac{E}{T}\right) \approx \exp\left(-\frac{E}{T_c}\right)\exp\vartheta\,. \quad (20)$$

At the cusp, $D = 1$ and $S = 4/Z$, where $Z = EQ/(cT_c^2)$ is the Zeldovich number, $\vartheta = 0$, and the heat bath temperature is $\vartheta_a = -2$. The convenient parameters to use in the neighborhood of this point are d and s such that $D = 1 + d$ and $S = (4/Z)(1 + s)$, in terms of which the boundary of the bistability region takes the form

$$s = \frac{d}{2} \pm \frac{2\sqrt{2}}{3}(-d)^{3/2}\,. \quad (21)$$

The straight line $s = d/2$ corresponds to phase equilibrium for $d < 0$ and is similar to a critical isochore for $d > 0$. On this line, as before, $\vartheta \approx 0$, and in the bistability region, $\vartheta \approx \pm\sqrt{-6d}$. On the spinodals, $\vartheta \approx \mp\sqrt{-2d}$.

As trajectories approach the limit point in the state space, they start oscillating in a random manner, covering quite a large region, a critical attractor. We examine the properties of such an attractor with the example of the system

$$\dot\eta = (1 - \eta)\exp\vartheta - \eta D^{-1}\,, \quad (22)$$

$$\dot\vartheta = Z(1 - \eta)\exp\vartheta - \frac{2 + \vartheta}{S} - \frac{2}{S}\,y(t)\,, \quad (23)$$

obtained from Eqns (13) and (14) using the transformations discussed above. The source of weak noise in Eqn (23) is turbulence in the reactor cooling system. Figure 1 shows a trajectory [19] in the (η, ϑ) plane for $D_c - 1 = 3 \times 10^{-4}$ and $S_c - 1 = 1.5 \times 10^{-4}$, demonstrating the shape and size of the critical attractor. In Fig. 2, a small portion of this plot is shown on an enlarged scale, demonstrating the Brownian nature of this trajectory.

5. Van der Waals and fluctuation regions

We linearize Eqn (16) in the vicinity of the minimum ϑ_0 to obtain

$$\ddot\vartheta_1 + \gamma_0\dot\vartheta_1 + \omega_0^2\vartheta_1 = 0\,, \quad (24)$$

where the time scale is $(1/k)\exp(E/T_c)$, $\vartheta_1 = \vartheta(t) - \vartheta_0$, $\gamma_0 = \gamma(\vartheta = \vartheta_0, \dot\vartheta = 0)$, and

$$\omega_0 = \left[\exp\vartheta_0\left(\frac{Z}{D} - \frac{3 + \vartheta_0}{S}\right) - \frac{1}{DS}\right]^{1/2}. \quad (25)$$

The frequency ω_0 vanishes at the cusp and is small near it (which implies a small value of the restoring force that occurs when the reactor deviates from the steady-state operation). A small excitation $\varepsilon\exp(-i\omega t)$ in the right-hand side of Eqn (24) produces a response $A\exp(-i\omega t)$. Defining the susceptibility $\sigma(\omega)$ as the ratio A/ε, we obtain

$$\mathrm{Re}\,\sigma = \frac{\omega_0^2 - \omega^2}{R}\,, \qquad \mathrm{Im}\,\sigma = \frac{\gamma_0\omega}{R}\,, \qquad R = (\omega_0^2 - \omega^2) + \gamma_0^2\omega^2\,. \quad (26)$$

With the right-hand side of Eqn (24) taken to be weak white noise, the Fourier components of the correlation function $\langle\vartheta_1(t)\,\vartheta_1(t')\rangle$ are found as

$$(\vartheta^2)_\omega = \rho\gamma_0^{-1}\,\frac{\mathrm{Im}\,\sigma}{\omega}\,, \quad (27)$$

where ρ is the frequency-independent spectral noise density (an analog of the fluctuation–dissipation theorem, with $\rho/2\gamma_0$ playing the role of temperature). The integral over spectrum (27) is the variance, and hence in the limit $\vartheta_0 \to 0$, all modes increase, but the soft one especially so. The closer the critical point is, the higher and sharper the low-frequency peak.

Equations (24)–(27) hold for what can be called the van der Waals region. In a sufficiently small neighborhood of the cusp, the nonlinearity is important. By analogy with Ginzburg's criterion [20], we can compare the variance of critical fluctuations $\langle\vartheta_1^2\rangle$ and the characteristic value $\vartheta_0^2 \sim |d|$ to determine the boundaries of this neighborhood. Nonlinear effects have been investigated in [21] by integrating system (22), (23) numerically. The weak noise in Eqn (23) may be due to turbulence in the reactor cooling system.

Figure 3 shows the variation of the variance $\langle\vartheta_1^2\rangle$ with $|d|$ on a log–log scale. For $d > 0$, i.e., outside the bistability region, we see that the initial power-law increase is followed by saturation. The critical exponent is, according to Eqn (27), -1, to be compared with the least-square value -0.99.

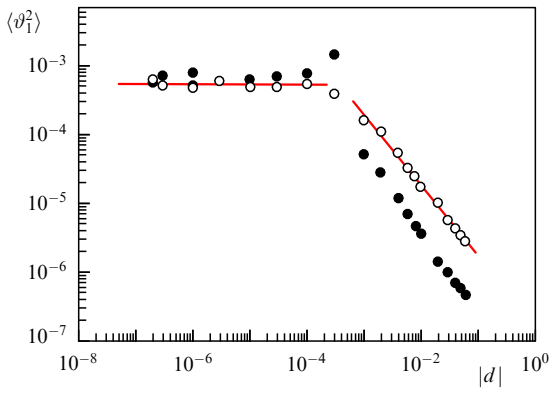

Figure 3. Temperature fluctuation variance as a function of the distance to the cusp: (○) $d > 0$, (●) $d < 0$. Straight lines are obtained by the least-square processing of the corresponding portion of the plot.

6. Kramers transitions

For $d < 0$, there is a variance peak between the van der Waals and fluctuation regions in the plot in Fig. 3. In the bistable region, the potential has two minima, with the barrier between them lowering with decreasing $|d|$. This allows spontaneous transitions between the minima [22] due to the noise-induced diffusion in the field $\mathrm{d}V/\mathrm{d}\vartheta$. The transition probability W obeys the Arrhenius law, which, in this particular case, has the form

$$W \propto \exp\left[-\frac{2\gamma_0}{\rho}(V_\mathrm{m} - V_{\mathrm{d,u}})\right]. \qquad (28)$$

Figure 4 shows a plot of $\vartheta(t)$ for two values of d of the same magnitude but opposite sign. For $d < 0$, along with critical pulsations, large temperature jumps are observed: instead of oscillations about one of the limit points in the (η, ϑ) plane, oscillations about another limit point in the same plane occur. A kind of intermittency is observed in the plot. Transitions between hot and cold states lead to a significant increase in the variance $\langle(\vartheta - \vartheta_0)^2\rangle$. As $|d| \to 0$, the difference $V_\mathrm{m} - V_{\mathrm{d,u}}$ decreases and the contribution from the jumps vanishes. As $|d|$ increases, probability (28) falls off exponentially, and no jumps occur during the computation run. Nonlinear effects in the bistability region are more pronounced due to the quadratic terms in the expansion of $\mathrm{d}V/\mathrm{d}\vartheta$ in powers of ϑ around the potential minimum (for $d > 0$, no such term is present). As can be seen from Fig. 3, this region also contains the interval of a power-law behavior $\langle\vartheta_1^2\rangle \propto |d|^{-n}$, but with an exponent noticeably larger than unity ($n \approx 1.2$).

Similar jumps in a bistable system are described in Ref. [23], which is concerned with stimulated oscillations of a micromechanical vibrator, with bistability due to an S-like nonlinear resonance curve. We also note the numerical simulation of fluctuations at the transition from one potential well to two [24] (where only one — single-minimum — phase was studied).

7. Limit cycle developing out of critical chaos

Unlike the critical point for transitions between phases of the same symmetry, system (22), (23) can have periodic solutions [25–27]. According to Eqn (16), the oscillatory instability boundary is determined by the conditions $\gamma(T = T_0, \dot{T} = 0) = 0$, where T_0 is the temperature of the steady-state regime under consideration. If the parameters vary along the straight line $s = d/2$ ($d > 0$), γ vanishes at $Z = Z_v \approx 8 + 2d^2$. Close to this threshold, for $Z = 8$, the pulse spectrum does not look qualitatively different from that

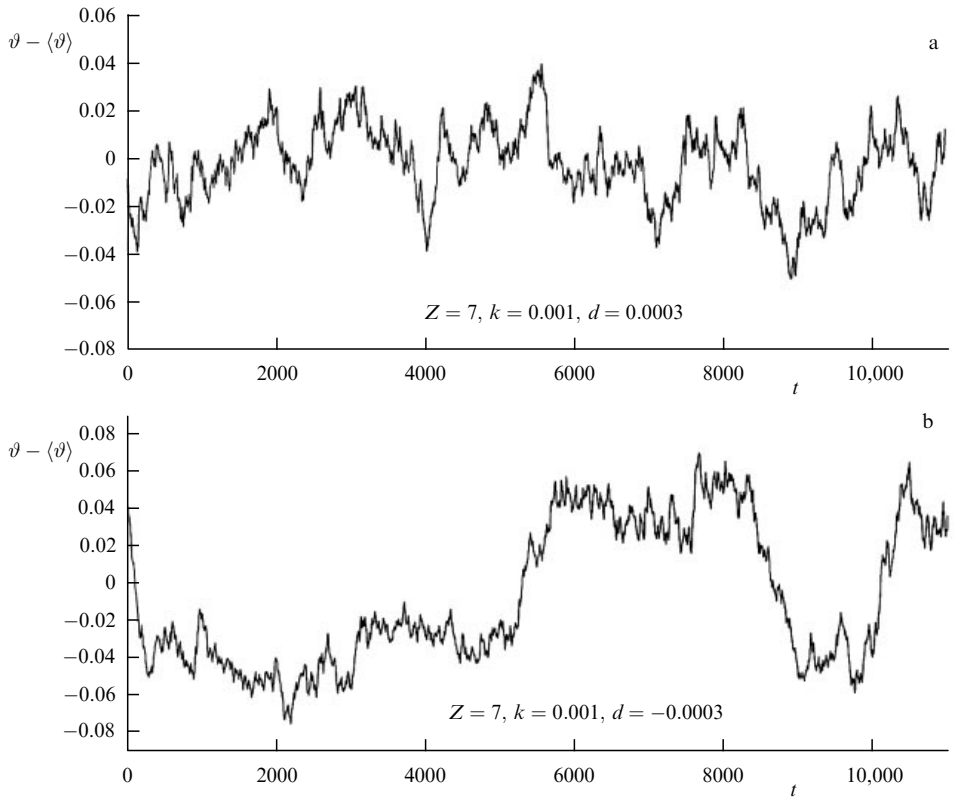

Figure 4. Example plots of the time dependence of temperature, $|d| = 3 \times 10^{-4}$: (a) $d > 0$, (b) $d < 0$.

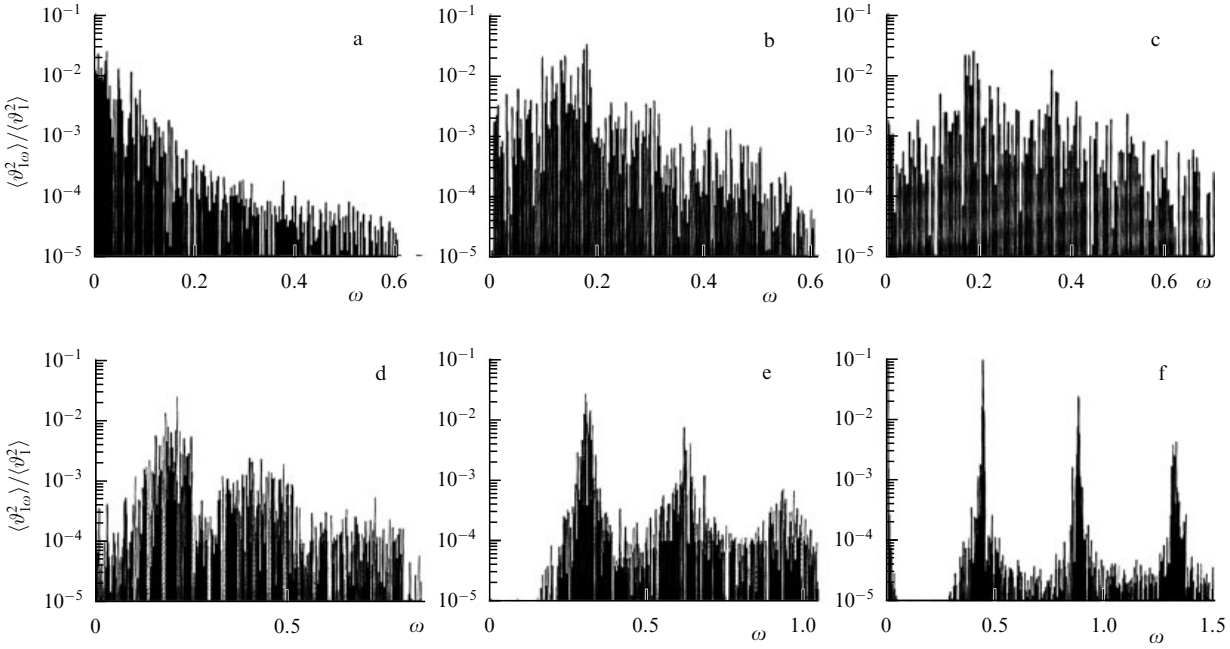

Figure 5. Frequency spectra for various values of Z: (a) 7, (b) 8, (c) 8.1, (d) 8.2, (e) 8.5, and (f) 9. Abscissa: $\omega = 2\pi n$, n are integers, t_0 is the computation time.

for $Z = 7$. Further evolution of the spectrum is illustrated in Fig. 5, which shows that the spectrum broadens at $Z = 8$, a small 'friction' causes the excitation of a large number of modes, but the spectrum remains continuous. The expansion continues at $Z = 8.1$, i.e, where the regime of regular oscillations would set in in the absence of noise. It is only at large values of Z, deep in the instability region, that peaks at the fundamental frequency and higher harmonics appear. The fact that the power of the continuous spectrum condenses into lines can be interpreted as a synchronization effect [28] or a classical analog of Bose–Einstein condensation. To see that this is indeed the case, we note that a state of a time-periodic system is characterized by a phase. Upon condensation, the number of particles (or quanta) in a given state is large, and the uncertainty relation for the number of particles and the phase imposes no significant restriction on how accurately the phase can be determined. A similar discussion on the macroscopic filling of long-wavelength modes at the expense of short-wavelength ones can be found in Ref. [29].

8. Traveling fronts and pulses near the propagation threshold

As an example of a distributed-parameter system, we consider a set of small CSTR systems interacting via diffusion and heat conduction. Instead of Eqns (22), (23), we now write

$$\dot{\eta} = L\Delta\eta + (1-\eta)\exp\vartheta - \eta D^{-1}\,, \tag{29}$$

$$\dot{\vartheta} = \Delta\vartheta + Z(1-\eta)\exp\vartheta - \frac{2+\vartheta}{S} - \frac{2}{S}\,y(t)\,, \tag{30}$$

where $\sqrt{(\chi/k)\exp(E/T_*)}$ is the length scale, χ is the heat diffusivity, L is the Lewis number (the ratio of diffusivity to heat diffusivity), and the scale temperature is chosen to be $T_* = T_a + Q/c$. The reactors can be arranged in the form of a chain or a membrane, and Δ is the one- or two-dimensional Laplace operator. For solitary waves along the chain, the boundary conditions for Eqns (29) and (30) can be written as

$$x = \pm\infty\,, \qquad \frac{\partial\eta}{\partial x} = \frac{\partial\vartheta}{\partial x} = 0\,. \tag{31}$$

We use a no-flow, $\tau \to \infty$ scenario to study a traveling front. With the noise $y(t)$ turned off in Eqn (30), such a front consists of three zones: heating, reaction, and cooling [30]. The reaction zone concentrates near the temperature maximum and is narrow compared to the other two. In the heating zone, the reaction can be neglected due to the insufficiently high temperature, and in the cooling zone, the original material is already used up. In the wave-comoving frame of reference, Eqns (29) and (30) are steady state, with $\partial/\partial t \to u\,\partial/\partial x$, where u is the wave velocity. We approximate the chemical source in Eqn (30) with the function $\delta(x)$, where x is the reaction zone coordinate, and replace Eqn (29) with the condition

$$u = u_0 \exp\vartheta_m\,, \tag{32}$$

where u_0 is the front velocity under no-loss conditions for $S \to \infty$ and ϑ_m is the maximum temperature. It is easily seen that problem (29)–(32) has two solutions: two branches of $u(S)$, the upper increasing and the lower decreasing with increasing S. This situation is clearly unstable. The threshold is located where the branches merge.

For the problem with a δ source, it is easy to write the nonsteady-state wave solution:

$$\frac{1}{2\sqrt{\pi L}}\int_0^t \frac{\varphi(t')}{\sqrt{t-t'}}\exp\left[-\frac{l^2(t',t)}{4L(t-t')}\right]\mathrm{d}t' = 1\,, \tag{33}$$

$$\frac{1}{2\sqrt{\pi}}\int_0^t \frac{\varphi(t')}{\sqrt{t-t'}}\exp\left[-\frac{l^2(t',t)}{4(t-t')} - \frac{t-t'}{S}\right]\mathrm{d}t' = 1 + Z\vartheta_m\,, \tag{34}$$

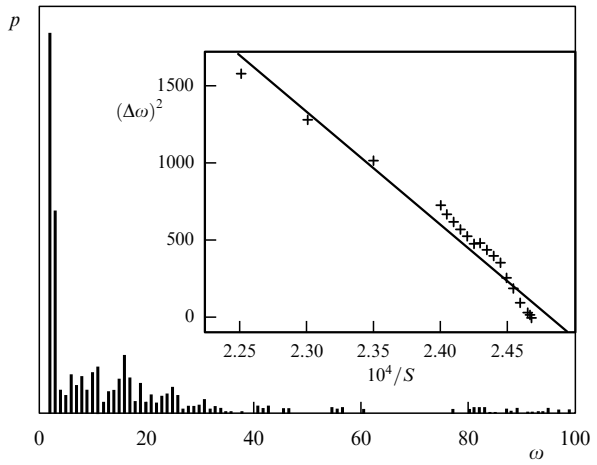

Figure 6. Typical pulsation spectrum $u(t) - \langle u \rangle$. Abscissa: the frequency $\omega = 2\pi n/t_0$, with n being an integer and $t_0 = 60{,}000$ the computation time. Inset: spectral maximum width versus distance to the threshold.

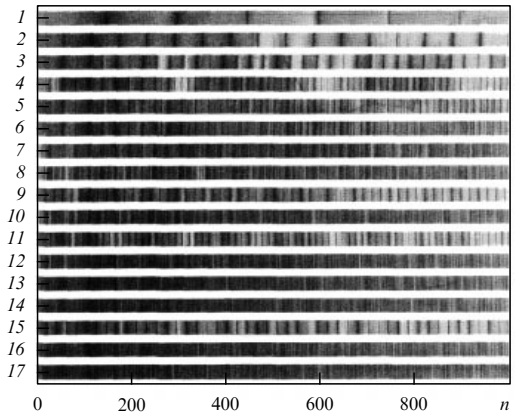

Figure 7. (See in color online.) Frequency spectra of the velocity pulsations as a function of $\omega = 2\pi n/t_0$, computation time $t_0 = 10^5$. The values of S: 350 (*1*), 328 (*2*), 326.914 (*3*), 326.640 (*4*), 326.620 (*5*), 326.611 (*6*), 326.551 (*7*), 326.500 (*8*), 326.466 (*9*), 326.400 (*10*), 326.375 (*11*), 326.350 (*12*), 326.315 (*13*), 326.250 (*14*), 326.230 (*15*), 326.219 (*16*), 326.213 (*17*). Discrete spectrum changes to continuous via intermittency.

where $\varphi^2 = u_0^2 \exp\vartheta_m$ and $l(t', t) = \int_{t'}^{t} u(t'')\,dt''$. In general, however, Eqns (33) and (34) are nonlinear integro-differential equations for u and ϑ_m, by no means easier to solve than the original problem. Near the threshold, the velocity varies slowly, allowing an expansion in the small parameter, which leads to the quasi-steady-state equation [31]

$$\frac{dv}{dt} = \frac{s - 2v^2}{t_*}, \qquad t_* = \frac{Z\sqrt{e}}{u_0^2}\left[L - 1 + \frac{2}{Z}(L+2)\right], \qquad (35)$$

where $v = u/u_{th} - 1$ and $s = S/S_{th} - 1$, with the index th denoting threshold values. Above the threshold, there are two steady-state points, the smaller of which is unstable; for $s < 0$, the velocity decreases and the wave decays. Because a realistic medium always contains at least small-size inhomogeneities and because the near-threshold susceptibility is high, the wave motion becomes chaotic. A point to note is the dominance of soft modes. The velocity fluctuation spectrum behaves as shown in Fig. 6.

The quasi-steady-state equation is in fact valid only for L close to unity. For $L > 1$, the planar front is unstable and becomes curved, whereas for $L < 1$, an oscillatory instability develops. Near the threshold, this instability produces random velocity pulsations in the absence of external noise (dynamical chaos). The period doubles as the parameter values shift to the threshold. The intervals between the doublings decrease as a geometric progression in accordance with Ref. [32]. The chaotic regimes are bounded by $S_* = 326.611$. The time dependence of the velocity shows an intermittent behavior between S_* and $S_{th} = 326.2$, as does the evolution of the frequency spectra with increasing S. Example spectra are shown in Fig. 7 [33].

If the flow transverse to the chain has a nonzero velocity, the solutions can be either switching waves between the hot and cold regions or traveling pulses. In the pulse after the reaction zone, the initial state restores itself due to the flow. Numerical simulations were performed for $L = 1$ [34]. It was found (Fig. 8) that as the parameters approach their threshold values, the time it takes for a pulse to attain the uniform motion regime increases, and oscillations occur. The oscillation period is large compared to the characteristic time $(1/k)\exp[E/(T_a + Qc^{-1})]$ and increases as $S \to S_{th}$. As

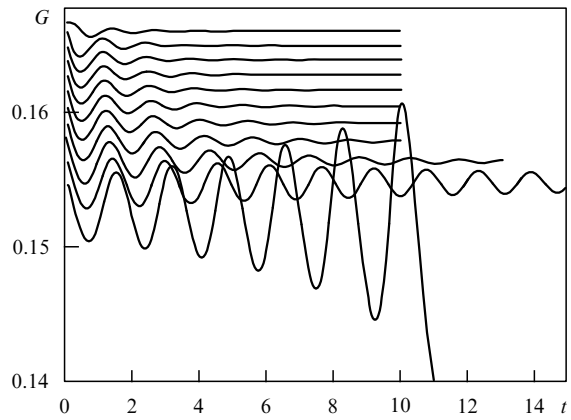

Figure 8. Time dependence of the pulse power (integral over the source) for S values close to the threshold. The top curve is constructed for $S = 770$, and each subsequent one, with S decreased by unity. For $S \leqslant 761$, the pulse decays irreversibly.

before, the dominance of soft modes near the bifurcation is seen.

9. Conclusions

The growth of soft modes near a bifurcation is a universal phenomenon. To study it, in addition to numerical simulation, real experiments were conducted [35] using an electrical circuit with a dinistor as a working element. This device, which exhibits an S-shaped current–voltage characteristic, was connected in series with a constant (current-independent) resistor R. The direct current regimes are determined by the intersection of the $I(V)$ characteristic and the loading straight line $I = (V_0 - V)/R$ (I is the current, V_0 is the applied voltage, and V is the voltage across the dinistor). Depending on the values of R and V_0, either one or three intersections are possible (with the middle one unstable in the latter case). For each R, V_0 pair, the variation of the pulsations of voltage V with time was recorded, with a recording time of 100 s. In total, 256 experimental runs were made. Example spectra are

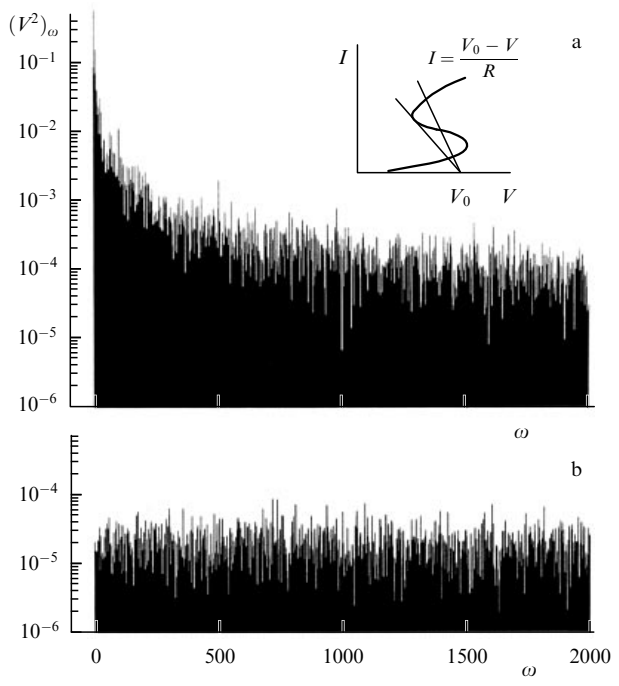

Figure 9. (See in color online.) Frequency spectra of pulsations close to and at a distance from the bifurcation point. (a) $R = 75$ kΩ, $V_0 = 30$ V, (b) $R = 60$ kΩ, $V_0 = 32$ V. Frequency is in units of $2\pi n/t_0$, t_0 is the duration of the experiment.

shown in Fig. 9. Far from the bifurcation, usual white noise is observed, but close to it, all the modes increase (the spectrum is normalized to the variance), but the soft modes especially so. At zero frequency, a maximum, or more precisely a resonance, forms.

The approach of a complex system (artificial or natural) to a bifurcation of its steady-state regime (i.e., to a catastrophe) can be predicted beforehand from the enhancement of soft modes in its noise spectrum, obviously motivating the development of spectrum-monitoring devices. The report by the Federal Service for Ecological, Technological and Atomic Surveillance (Rostechnadzor) on the Sayano-Shushenskaya hydroelectric station accident (for the online version, visit http://www.scientific.ru/trv/archive/act.doc) contains only one plot of the vibration amplitude for the turbine bearing cover. What happened in the accident was that the cover broke off and water rushed in to flood the station engine hall. During the observation period, the average value of the amplitude increased threefold, and its maximum value increased fifteenfold. As the report states, no resonances were detected, implying that the difference between the average and maximum values is due to the compression of the spectrum (zero frequency resonance, as discussed above). The term 'catastrophe precursors' is used in [36] in referring to soft modes. In an alternative 'compressive sensing' approach [37] for predicting catastrophes, unknown equations are restored from experimental data (time series). The right-hand side of each equation is written as an expansion in powers of dependent variables, with the expansion coefficients calculated by a computer program (most of them, incidentally, turn out to be negligibly small). But as the description in Ref. [37] implies, this procedure is realistic only for a small number of degrees of freedom (or the number of equations), not to mention distributed systems. By contrast, the method we propose here is simple and has no such restrictions, and we see it as our duty that it be made known as widely as possible throughout the science and technology community.

Acknowledgments

This paper was supported by the Russian Foundation for Basic Research Grant 11-03-00058-a and by the Russian Academy of Sciences Presidium program P-02, subprogram 1, code 2114.

References

1. Landau L D, Lifshitz E M *Statistical Physics* Vol. 1 (Oxford: Pergamon Press, 1980) [Translated from Russian: *Statisticheskaya Fizika* Vol. 1 (Moscow: Fizmatlit, 1995)]
2. Ornstein L S, Zernike F *Proc. Acad. Sci. Amsterdam* **12** 793 (1914)
3. Weissman M B *Rev. Mod. Phys.* **60** 537 (1988)
4. Langevin P *C.R. Acad. Sci.* **146** 530 (1908) [Translated into Russian: *Izbrannye Trudy* (Selected Works) (Moscow: Izd. AN SSSR, 1960) p. 338]
5. Lorenz E N *J. Atmos. Sci.* **20** 130 (1963)
6. Poincaré H *Sur les propriétés des fonctions définies par les équations aux différences partielles* (Paris: Gauthier-Villars, 1879) [Translated into Russian: *Izbrannye Trudy* (Selected Works) Vol. 1 *Novye Metody Nebesnoi Mekhaniki* (New Methods of Celestial Mechanics) (Moscow: Nauka, 1971)]
7. Arnol'd V I *Sov. Phys. Usp.* **26** 1025 (1983) [*Usp. Fiz. Nauk* **141** 569 (1983)]
8. Arnold V I *Catastrophe Theory* 3rd ed. (Berlin: Springer-Verlag, 1992) [Translated from Russian: *Teoriya Katastrof* 5th ed. (Moscow: URSS, 2007)]
9. Whitney H *Ann. Math.* **62** 374 (1955)
10. Loskutov A *Phys. Usp.* **53** 1257 (2010) [*Usp. Fiz. Nauk* **180** 1305 (2010)]
11. Sagdeev R Z, Usikov D A, Zaslavsky G M *Nonlinear Physics. From the Pendulum to Turbulence and Chaos* (Chur: Harwood Acad. Publ., 1988); Zaslavsky G M, Sagdeev R Z *Vvedenie v Nelineinuyu Fiziku. Ot Mayatnika do Turbulentnosti i Khaosa* (Introduction to Nonlinear Physics. From the Pendulum to Turbulence and Chaos) (Moscow: Nauka, 1988)
12. Binney J J et al. *The Theory of Critical Phenomena. An Introduction to the Renormalization Group* (Oxford: Clarendon Press, 1998)
13. Ivleva T P et al. *Chem. Eng. J.* **168** 1 (2011)
14. Frank-Kamenetskii D A *Acta Physicochim. USSR* **10** 365 (1939); *Zh. Fiz. Khim.* **13** 738 (1939)
15. Zel'dovich Ya B *Zh. Tekh. Fiz.* **11** 493 (1941)
16. Rumanov É N *Dokl. Phys.* **51** 238 (2006) [*Dokl. Ross. Akad. Nauk* **408** 325 (2006)]
17. Van der Pol B *Radio Rev.* **1** 701 (1920)
18. Merzhanov A G, Rumanov É N *Sov. Phys. Usp.* **30** 293 (1987) [*Usp. Fiz. Nauk* **151** 553 (1987)]
19. Vaganova N I, Rumanov E N *Dokl. Phys.* **56** 507 (2011) [*Dokl. Ross. Akad. Nauk* **440** 463 (2011)]
20. Ginzburg V L *Sov. Phys. Solid State* **2** 1824 (1961) [*Fiz. Tverd. Tela* **2** 2031 (1960)]
21. Vaganova N I, Rumanov É N *JETP* **108** 349 (2009) [*Zh. Eksp. Teor. Fiz.* **135** 395 (2009)]
22. Kramers H A *Physica* **7** 284 (1940)
23. Chan H B, Stambaugh C *Phys. Rev. Lett.* **99** 060601 (2007)
24. Kravtsov Yu A, Surovyatkina E D *Phys. Lett. A* **319** 348 (2003)
25. Frank-Kamenetskii D A , Sal'nikov I E *Zh. Fiz. Khim.* **17** 79 (1943)
26. Aris R, Amundson N R *Chem. Eng. Sci.* **7** 121 (1958)
27. Vaganov D A, Samoilenko N G, Abramov V G *Chem. Eng. Sci.* **33** 1131 (1978)
28. Pikovsky A, Rosenblum M, Kurths J *Synchronization. A Universal Concept in Nonlinear Sciences* (Cambridge: Cambridge Univ. Press, 2001) [Translated into Russian (Moscow: Tekhnosfera, 2003)]
29. Keldysh L V, Tikhodeev S G *Sov. Phys. JETP* **64** 45 (1986) [*Zh. Eksp. Teor. Fiz.* **91** 78 (1986)]
30. Zel'dovich Ya B *Zh. Eksp. Teor. Fiz.* **11** 159 (1941)
31. Dovzhenko A Yu, Maklakov S V, Rumanov I E, Rumanov E N *JETP* **95** 973 (2002) [*Zh. Eksp. Teor. Fiz.* **122** 1125 (2002)]

32. Feigenbaum M J *J. Stat. Phys.* **19** 25 (1978)
33. Dovzhenko A Yu, Rumanov É N *JETP* **98** 359 (2004) [*Zh. Eksp. Teor. Fiz.* **125** 406 (2004)]
34. Dovzhenko A Yu, Rumanov É N *JETP* **104** 508 (2007) [*Zh. Eksp. Teor. Fiz.* **131** 567 (2007)]
35. Dovzhenko A Yu, Dovzhenko M, Mashkinov L B, Rumanov É N *Dokl. Phys.* **48** 13 (2003) [*Dokl. Ross. Akad. Nauk* **388** 181 (2003)]
36. Rumanov E N, Vaganova N I *Priroda* (10) 23 (2011)
37. Wang W-X et al. *Phys. Rev. Lett.* **106** 154101 (2011)